N-myristoylation determines dual targeting of mammalian NADH-cytochrome b(5) reductase to ER and mitochondrial outer membranes by a mechanism of kinetic partitioning

Sara Colombo,[1] Renato Longhi,[2] Stefano Alcaro,[3] Francesco Ortuso,[3] Teresa Sprocati,[1] Adriano Flora,[1] and Nica Borgese[1,3]

[1]Consiglio Nazionale delle Ricerche Institute of Neuroscience, Cellular and Molecular Pharmacology Section and Department of Medical Pharmacology, University of Milan, 20129 Milan, Italy
[2]Consiglio Nazionale delle Ricerche Institute of Chemistry of Molecular Recognition, 20133 Milan, Italy
[3]Department of Pharmacobiology, University of Catanzaro, 88021 Roccelletta di Borgia (Catanzaro), Italy

Mammalian NADH-cytochrome b(5) reductase (b5R) is an N-myristoylated protein that is dually targeted to ER and mitochondrial outer membranes. The N-linked myristate is not required for anchorage to membranes because a stretch of hydrophobic amino acids close to the NH_2 terminus guarantees a tight interaction of the protein with the phospholipid bilayer. Instead, the fatty acid is required for targeting of b5R to mitochondria because a nonmyristoylated mutant is exclusively localized to the ER. Here, we have investigated the mechanism by which N-linked myristate affects b5R targeting. We find that myristoylation interferes with interaction of the nascent chain with signal recognition particle, so that a portion of the nascent chains escapes from cotranslational integration into the ER and can be post-translationally targeted to the mitochondrial outer membrane. Thus, competition between two cotranslational events, binding of signal recognition particle and modification by N-myristoylation, determines the site of translation and the localization of b5R.

Introduction

Although many newly synthesized polypeptides are delivered to a single organelle with a high degree of accuracy, some proteins follow dual or multiple targeting pathways and thus reside in more than one compartment within the cell. Differently localized protein forms are often variants that derive from processes of alternative splicing, alternative promoter utilization, or translation from alternative initiation codons, but there are also cases in which a single primary translation product follows more than one targeting pathway (for review see Danpure, 1995) because of the coexistence of competing targeting signals within the same polypeptide chain. Because proteins in different locations may interact with different partners, multiple protein targeting has potentially important functional implications.

Mitochondria and the ER offer an example of two compartments specialized for different functions, which each possess their unique complement of polypeptides, yet do share some protein components. For instance, some members of the bcl-2 family, including bcl-2 itself, localize both to the ER and to the mitochondrial outer membrane (MOM), and it is thought that on these two different membranes they regulate apoptosis through distinct mechanisms (for review see Adams and Cory, 2001). Because mitochondria and ER are not connected by vesicular traffic, the dual localization of these proteins implies that they engage two distinct targeting machineries.

Another example of a protein localized to both the MOM and the ER membrane is the mammalian membrane-bound form of the flavoprotein NADH-cytochrome b(5) reductase (b5R; for review see Borgese et al., 1993), whose deficit is responsible for a rare but incapacitating genetic disease, type II hereditary methemoglobinemia (Jaffé and Hultquist, 1995; Shirabe et al., 1995). A single cDNA, coding for the wild-type

Correspondence to Nica Borgese: n.borgese@in.cnr.it

A. Flora's present address is Baylor College of Medicine, Houston, TX 77030.

Abbreviations used in this paper: b5R, NADH-cytochrome b(5) reductase; CD, circular dichroism; DPM, dog pancreas microsomes; DSS, disuccinimidylsuberate; GAPDH, glyceraldehyde phosphate dehydrogenase; MOM, mitochondrial outer membrane; MyrCoA, myristoyl-CoA; NMT, N-myristoyl-CoA:protein myristoyltransferase; RNC, ribosome-nascent chain complex; SRP, signal recognition particle; TFE, trifluoroethanol; wt, wild-type.

The online version of this article includes supplemental material.

The Journal of Cell Biology, Vol. 168, No. 5, February 28, 2005 735–745
http://www.jcb.org/cgi/doi/10.1083/jcb.200407082

(wt) enzyme from a unique start codon, produces a protein with the dual ER/MOM localization in transfected cells, indicating that the same translation product interacts with mitochondrial and ER targeting machinery (Borgese et al., 1996). On the two membranes b5R carries out different functions: on the ER, via its electron acceptor cytochrome b(5), it participates in diverse aspects of lipid metabolism, (for review see Borgese et al., 1993); on the MOM instead it mediates the regeneration of ascorbate from ascorbate free radical (Ito et al., 1981), but may also be involved in more fundamental aspects of mitochondrial physiology, such as the transfer of electrons from cytosolic NADH to cytochrome *c* in the intermembrane space (Bernardi and Azzone, 1981).

Like members of the bcl-2 family, most of the mass of b5R, comprising its FAD and NADH binding domains, is exposed to the cytosol. However, whereas bcl-2 proteins are C-tail anchored, b5R is bound to the bilayer by a short anchor at its NH_2 terminus. This region consists of a moderately hydrophobic stretch of 14 amino acids preceded by a myristoylation consensus sequence (see Fig. 1). The NH_2-terminal glycine of the membrane-bound form of b5R is indeed myristoylated (Ozols et al., 1984), and this modification is present in a 1:1 molar ratio to protein in both the MOM- and the ER-associated forms (Borgese and Longhi, 1990). N-myristoylation is a cotranslational, generally irreversible modification that is often necessary, although not sufficient, for membrane binding of the modified protein (for review see Resh, 1999). In the case of b5R, however, myristoylation does not detectably alter the strength of the enzyme's association with phospholipid bilayers because the 14-residue-long hydrophobic stretch is sufficient to tightly anchor the nonmyristoylated form to both artificial (Strittmatter et al., 1993) and ER membranes (Borgese et al., 1996). Myristoylation also does not affect the catalytic activity of the enzyme (Strittmatter et al., 1993; Borgese et al., 1996). Instead, this modification has a pronounced effect on targeting of b5R because the nonmyristoylated mutant (in which the acceptor Gly is mutated to Ala) is no longer delivered to mitochondria and localizes exclusively to the ER in cultured mammalian cells (Borgese et al., 1996). Thus, in the case of b5R, N-linked myristate appears to have a specific role in targeting rather than functioning simply as a membrane anchor.

Here, we have investigated the mechanism by which myristoylation affects targeting of b5R. We find that, in the absence of myristoylation, the NH_2-terminal sequence functions as a signal anchor that interacts with signal recognition particle (SRP) and is cotranslationally inserted into the ER. Myristoylation of the NH_2 terminus lowers the affinity of the interaction with SRP so that a portion of the nascent chains remains on free polysomes and becomes available for post-translational targeting to the MOM. Our results show that competition between two cotranslational events—myristoylation and SRP binding—can result in dual localization of a protein by a mechanism of kinetic partitioning.

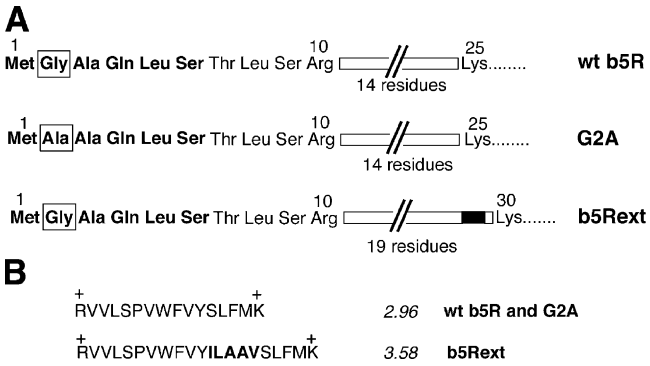

Figure 1. **Schematic representation of the NH_2-terminal regions of the three constructs used in this study.** (A) The residues that constitute the myristoylation consensus are in boldface, the Gly that accepts the myristoyl moiety is boxed. This residue is mutated to Ala in G2A b5R. The rectangle downstream to Arg10 represents the hydrophobic region in all three constructs; this region is lengthened by five residues (filled part of the rectangle) in b5Rext. (B) Amino acid sequence (one-letter code) of the hydrophobic region (flanked by a basic residue on both sides) of the three constructs. The residues inserted in b5Rext are shown in boldface. The average hydrophobicity of the 12 residues after Arg10 was calculated according to the STA PRIFT scale (Cornette et al., 1987), and is displayed in italics to the right of the sequences.

Results

Characterization of b5R constructs stably expressed in MDCK cells

In previous work (Borgese et al., 1996) we reported that a nonmyristoylatable G2A mutant of b5R looses the dual MOM/ER localization of the wt myristoylated protein, while remaining capable of tightly binding to the ER membrane, thanks to the 14-residue-long hydrophobic stretch close to the NH_2 terminus (between R10 and K25; see Fig. 1). In the present work, we also investigated how increased hydrophobicity of the membrane-anchoring region would affect targeting of b5R. Therefore, we created a second mutant, b5Rext, in which the myristoylation consensus is maintained but the length and hydrophobicity of the downstream region is increased by addition of five amino acids (ILAAV) between Y20 and S21 (Fig. 1). Stably transfected MDCK lines, expressing each of the three constructs, had similar levels of enzyme activity, indicating that alteration of the anchoring moiety does not impair the folding or the membrane topology of the enzyme (Fig. S1 A, available at http://www.jcb.org/cgi/content/full/jcb.200407082/DC1).

We compared the intracellular localization of the three constructs in the cell lines by confocal analysis (Fig. 2). b5R was undetectable by immunofluorescence in nontransfected MDCK cells under the conditions used (not depicted). As previously reported, the transfected wt protein colocalized with markers both of mitochondria (Fig. 2 A, a–c) and of the ER (Fig. 2 B, a–c), whereas the G2A mutant localized to the ER (Fig. 2 B, d–f), but not to mitochondria (Fig. 2 A, d–f). A similar distribution, with no antigen detectable on mitochondria, was seen for the b5Rext mutant (Fig. 2, A and B; g–i). We confirmed the lack of mitochondrial localization for b5Rext also by cell fractionation (Fig. S1 B). Thus, the effect of elimination of myristoylation (in G2A) and of increasing the length/hydrophobicity of the membrane anchor (in b5Rext) similarly abolished mitochondrial targeting of b5R.

To further characterize the constructs, we investigated their myristoylation status by metabolic labeling with ^{3}H-myristic acid or ^{35}S-Met/cys in parallel dishes, followed by immunoprecipitation. As expected, the G2A mutant, although present, was not myristoylated (Fig. 3 A, lane 2 in top and

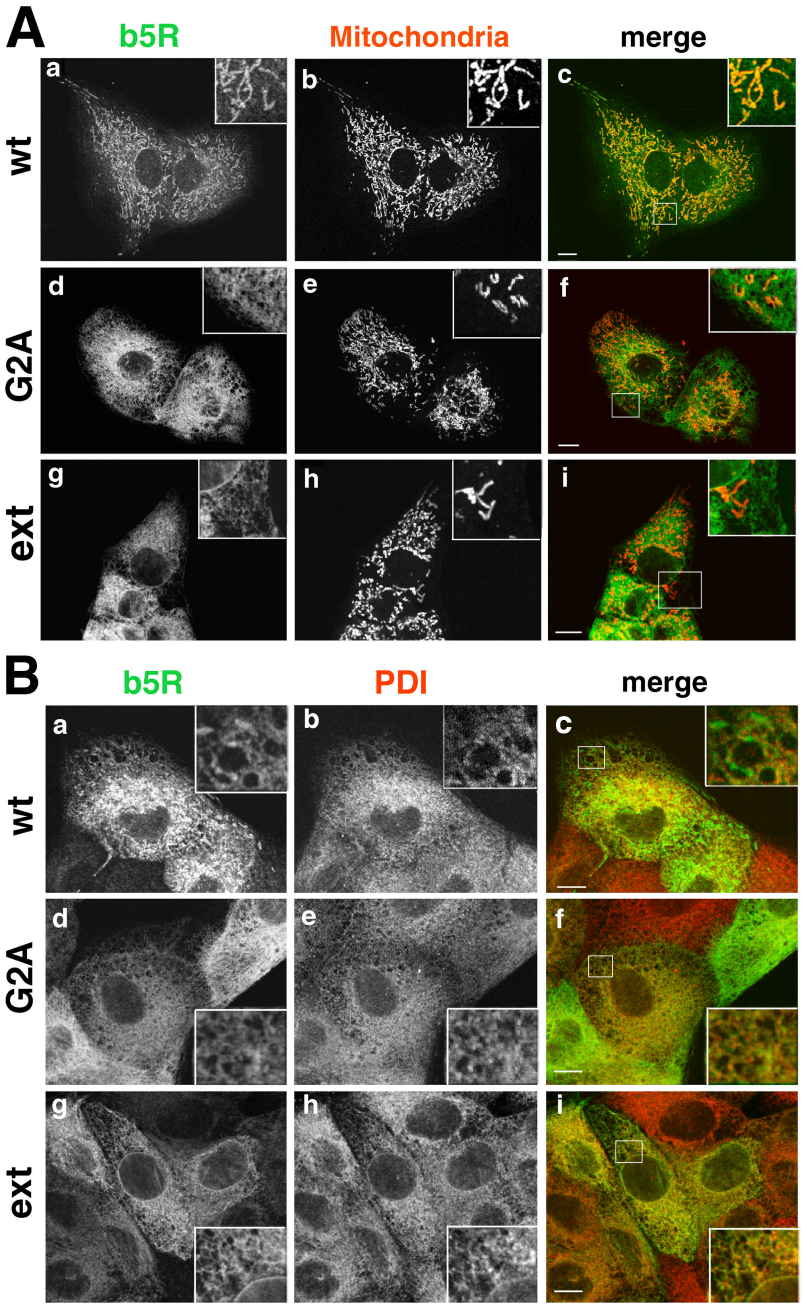

Figure 2. **Dual localization of wt b5R, and ER-restricted distribution of G2A and b5Rext mutants, in stably transfected MDCK cells.** Cells expressing each of the three proteins, as indicated to the left of the panels, were doubly stained with goat anti-b5R antibodies, followed by biotinylated anti–goat IgG and AlexaFluor 488–conjugated streptavidin (a, d, and g in A and B), and polyclonal anti-complex III antibodies or anti-protein disulfide isomerase (PDI) antibodies (b, e, and h in A and B respectively), both followed by Texas red–conjugated anti–rabbit IgG. In the merged images (shown in c, f, and i of both panels), the yellow color indicates colocalization. wt b5R colocalizes with the mitochondrial marker, but in addition shows a more widespread distribution (A), due to its ER localization demonstrated by colocalization with PDI (B). G2A and b5Rext do not show colocalization with the mitochondrial marker (A), but extensively colocalize with PDI (B). Bars, 10 μm. The closed boxes in the merged images indicate the area that is enlarged in the corresponding inset.

bottom), whereas both the wt and extended mutant of b5R incorporated the labeled fatty acid (Fig. 3 A, lanes 1 and 3). However, when the degree of myristoylation of these two constructs was evaluated by the ratio of ^{3}H to ^{35}S radioactivity, we consistently found that b5Rext was myristoylated with <40% the efficiency of the wt protein (Fig. 3 B).

Distribution of mRNA coding for b5R constructs in stably expressing MDCK cells

ER membrane proteins with b5R's topology are generally inserted cotranslationally because their NH_2-terminal hydrophobic domain interacts with SRP (Goder and Spiess, 2001). On the other hand, MOM proteins are targeted post-translationally (Shore et al., 1995), and early studies (Borgese and Gaetani, 1980; Okada et al., 1982) reported that in liver, b5R is synthesized on free polyribosomes, suggesting that its insertion into both the ER and the MOM is a post-translational event. As a first step to elucidate the in vivo–targeting pathways of our constructs, we analyzed by Northern blotting the distribution of the corresponding mRNAs between free and bound polysome fractions prepared from the transfected MDCK cell lines. In three separate experiments, we observed that all three transcripts were recovered in the bound polysome fraction, but that the mRNA specifying wt b5R was present also in the free fraction, at a concentration equal to 20–30% of that in bound polysomes; for the transcripts specifying the two mutant b5Rs the corresponding percentage was ~5 (Fig. 4 A, third panel from top).

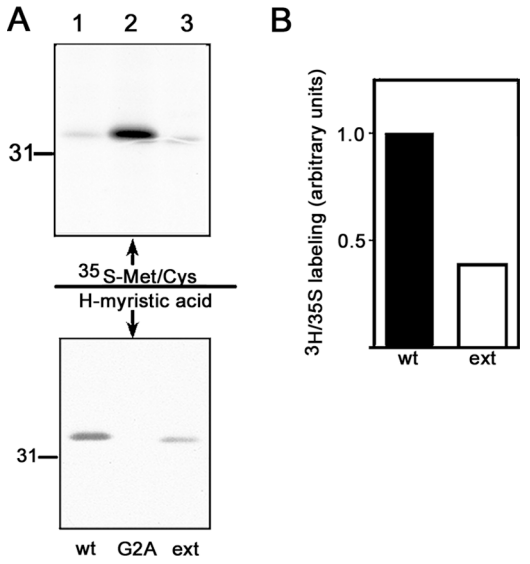

Figure 3. **Analysis of myristoylation of b5R forms by metabolic labeling.** MDCK cells expressing the indicated b5R forms were incubated with either 0.1 mCi/ml of ^{35}S-Promix for 3 h (top) or 0.1 mCi/ml of ^{3}H-myristic acid for 6 h. b5R was immunoprecipitated from the detergent lysates and analyzed by 11% SDS-PAGE fluorography. Both wt b5R (lane 1) and its extended mutant (lane 3) are myristoylated, whereas G2A (lane 2) is not. The position of the 31-kD size marker is shown. (B) b5Rext is less efficiently myristoylated than the wt protein. The band intensities of the gels of B were quantified by scanning. The ^{3}H/^{35}S ratio for wt b5R was arbitrarily set to 1.

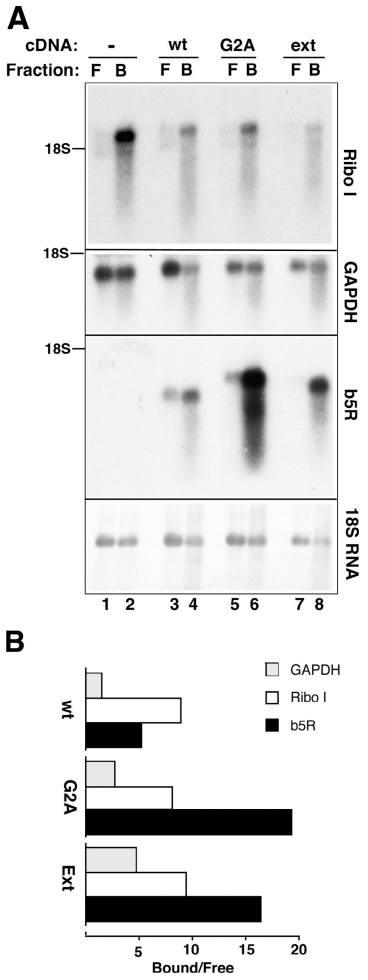

Figure 4. **b5R mRNA is distributed on both free and bound polysomes, whereas mutant transcripts are translated exclusively on bound polysomes.** (A) Blot analysis of RNA extracted from free (F) and bound (B) polysome fractions prepared from nontransfected MDCK (lanes 1 and 2) or from cells stably transfected with wt b5R (lanes 3 and 4), G2A (lanes 5 and 6), and b5Rext (lanes 7 and 8). 3.6 μg RNA from free and 1.8 μg from the bound polysomes were loaded. The blot was stained with methylene blue and then sequentially hybridized with probes for ribophorin I, GAPDH, and b5R as indicated. The bottom panel shows the methylene blue–stained 18S ribosomal RNA. The position of the 18S RNA in all panels is indicated. (B) Quantification by phosphorimaging of the signals of the experiment illustrated in A. The ratios of the intensities of the signal in the bound versus the free polysome fraction are shown after correction for the different RNA loads.

The distribution of the endogenous b5R mRNA in nontransfected cells (visible after longer exposure times not depicted in Fig. 4) was similar to that of the transfected wt b5R.

To exclude that the difference between the distributions of wt b5R and mutant transcripts was due to a different fractionation behavior of the polysomes in the different cell lines, we compared the b5R mRNA distribution with that of mRNAs for ribophorin I, a cotranslationally inserted type I membrane protein (Harnik-Ort et al., 1987), and for glyceraldehyde phosphate dehydrogenase (GAPDH), a cytosolic enzyme, as markers for transcripts translated on bound and free polysomes, respectively. As shown in Fig. 4 A (top) and Fig. 4 B, ribophorin mRNA, although partially degraded, was highly enriched in the bound versus the free polysome fraction. GAPDH mRNA (Fig. 4 A, second panel, and Fig. 4 B) was present in both fractions, indicating that bound polysomes were contaminated by free polysomes. In addition, the relatively low concentration of GAPDH mRNA in the free polysome preparation can be explained by the presence of inactive ribosomes in this fraction. Importantly for our investigation, the b5R mRNAs coding for the G2A and b5Rext mutants were even more enriched in the bound polysome fraction than ribophorin I mRNA (presumably because they are less degraded), whereas mRNA coding for wt b5R had a distribution intermediate between that of ribophorin I and GAPDH transcripts, indicating its presence in both the free and bound polysome populations (Fig. 4 B). The discrepancy with previous publications, which reported exclusive localization of hepatic b5R mRNA to free polysomes (Borgese and Gaetani, 1980; Okada et al., 1982), is presumably due to differences both in the cell type and the methodology used in those studies.

b5R nascent chains interact with SRP in vitro

The above results suggest that myristoylation can interfere with recruitment of polysomes to the ER membrane. This could occur at either of the two steps involved in cotranslational translocation/integration of proteins, i.e., signal sequence interaction with SRP and/or its engagement of the translocation channel at the ER membrane (Belin et al., 1996; Kim and Hegde, 2002). To distinguish between these two possibilities, and to investigate the cause of the low efficiency of myristoylation of the b5Rext mutant, we turned to in vitro translation experiments.

In the wheat germ extract, addition of SRP in the absence of microsomal membranes slows down elongation of signal

peptide bearing nascent chains (Walter and Blobel, 1983b), and this effect can be exploited to probe for signal peptide–SRP interaction. First, we analyzed the effect of high concentrations (100 nM) of SRP on the in vitro translation of b5R mRNAs. As control, we used a transcript coding for a soluble form of the enzyme, which lacks the entire hydrophobic NH_2-terminal domain (Pietrini et al., 1992). As seen in Fig. 5 A, translation of all three membrane-binding constructs of b5R was blocked under these conditions, whereas the translation of the soluble form was much less affected (lanes 7 and 8). Thus, the NH_2-terminal domain of b5R can indeed be defined as an SRP-interacting signal anchor.

Then we determined the concentration dependence of the SRP effect for the three constructs (Fig. 5, B and C). The mRNA for the soluble protein luciferase (Promega) was included in all samples as internal standard. Fig. 5 B illustrates a typical experiment, and Fig. 5 C reports the quantification of the data from a large number of experiments. Translation of b5Rext was more sensitive to SRP than that of the other two constructs, consistently with its predicted higher affinity caused by the higher hydrophobicity of its signal-anchor (Ng et al., 1996). In these experiments, no significant difference was detected between wt and G2A b5R translation.

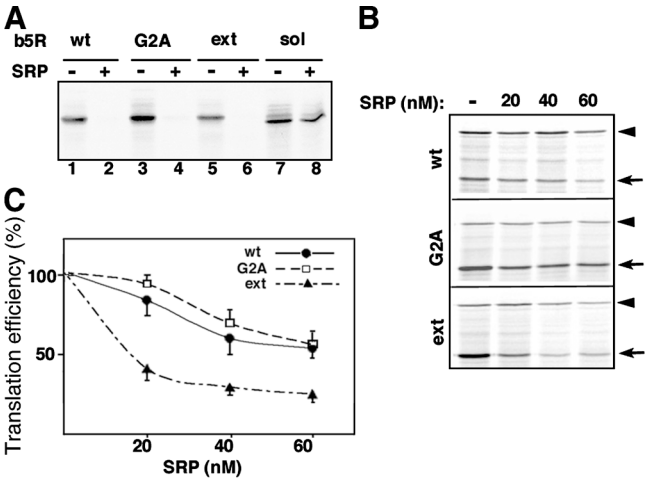

Figure 5. **b5R and its mutant forms interact with SRP.** (A) Synthetic transcripts coding for the indicated b5R forms were translated in wheat germ extract for 20 min in the absence or presence of 100 nM SRP, and analyzed by 11% SDS-PAGE autoradiography. SRP inhibits translation of the wt, G2A, and extended b5R (lanes 1–6), while having much less effect on the translation of a soluble b5R form that lacks the hydrophobic anchor (sol, lanes 7 and 8). (B) Dependence of translational slow-down on SRP concentration. wt b5R (top), G2A (middle), and b5Rext (bottom) transcripts were translated together with luciferase mRNA for 40 min in the presence of the indicated concentrations of SRP, and were analyzed by 11% SDS-PAGE phosphorimaging. The arrow and arrowhead indicate b5R and luciferase, respectively. (C) The intensities of the bands in six different experiments like the one shown in B were quantified. For each b5R form and in each experiment, the ratio of intensities of b5R to luciferase in the absence of SRP was set to 100% translation efficiency. Shown are averages with SEM.

Myristoylation interferes with SRP interaction in vitro

The comparable interaction of wt and G2A b5R nascent chains with SRP could have been due either to a lack of effect of N-myristoylation on this interaction or to low or no myristoylation occurring in vitro. Although the wheat germ extract is equipped with the enzymes required for N-myristoylation (Deichaite et al., 1988), the concentration of endogenous Myristoyl-CoA (MyrCoA) in the extract provided by Promega could be insufficient to support the reaction. When ^{3}H-MyrCoA was included in the translation mixes (prepared with unlabeled Met), wt b5R and the extended mutant were myristoylated, whereas G2A b5R was not (Fig. 6 A). To obtain a quantitative estimate of the degree of in vitro myristoylation of wt b5R, ^{35}S-Met and ^{3}H-MyrCoA of known specific activities were included together in the same incubation. After SDS-PAGE and blotting onto nitrocellulose, the radioactive b5R band was excised, solubilized, and counted in double label mode. From the ^{3}H/^{35}S ratio and the known methionine content of b5R, we were able to calculate the amount of added myristic acid attached to the in vitro–synthesized protein. As seen in Fig. 6 B, the calculated ratio increased with increasing concentration of MyrCoA, reaching a value of $\sim$1 at 120 μM MyrCoA. We could not test the effect of higher concentrations of MyrCoA because they interfered with in vitro translation. However, because a 1:1 stoichiometry of myristic acid to protein is the maximum value attainable, the result indicates that MyrCoA endogenous to the wheat germ extract does not significantly contribute to the reaction. Thus, the MyrCoA concentration in these extracts appears to be low, and limiting for the myristoylation reaction.

With the same methodology, we compared the degree of in vitro myristoylation of wt and b5Rext. In contrast to the in vivo situation, in vitro, in the absence of added SRP, the two constructs were myristoylated to the same extent (Fig. 6 C), indicating that the myristoylation consensus sequence is fully functional in the extended mutant, and that the lower degree of in vivo myristoylation may be due to its more efficient sequestration by SRP.

In light of the above results, we investigated the effect of MyrCoA on the interaction of SRP with b5R nascent chains. To this end, the degree of inhibition of b5R translation by a fixed concentration of SRP (50 nM) was evaluated at different concentrations of MyrCoA (Fig. 6 D). Again, in the absence of MyrCoA, SRP inhibited the translation of all three constructs but was most effective on b5Rext. Addition of MyrCoA had little or no effect on the SRP effect in the case G2A and b5Rext's translation while it reduced, in a dose-dependent manner, the wt protein's sensitivity to the SRP-induced translational slow-down.

To confirm the above results, we directly investigated the interaction of b5R nascent chains with SRP by cross linking. For these experiments, we tested the interaction of translated truncated mRNAs, coding for the NH_2-terminal portion of the three b5R forms, with the SRP endogenous to rabbit reticulocyte lysate. Preliminary experiments showed that, also in this system, endogenous MyrCoA is limiting because addition of this fatty acylCoA stimulated the translation of wt b5R, but not of G2A transcript (unpublished data). After translation of the truncated mRNAs in the presence or absence of MyrCoA, the ribosome-nascent chain complexes (RNCs) were isolated by ultracentrifugation through a high salt sucrose cushion

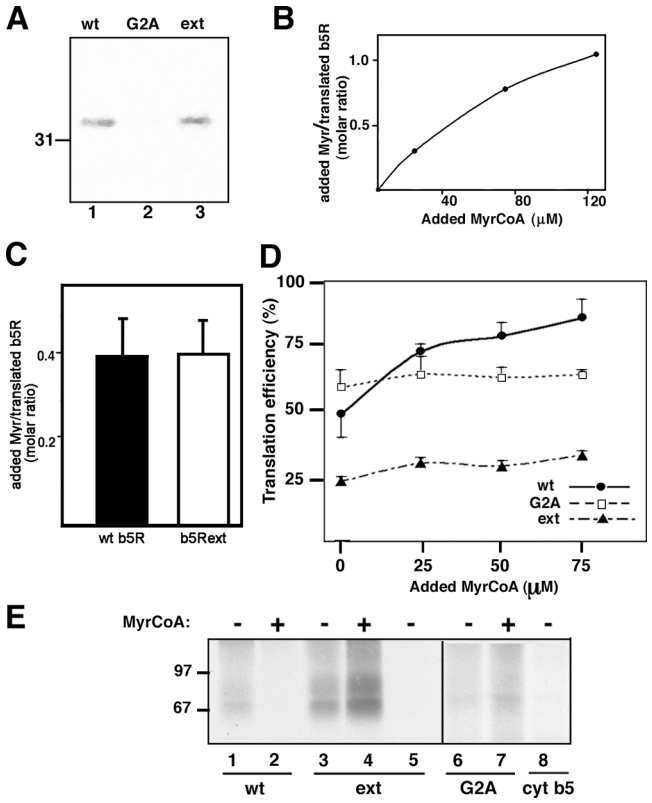

Figure 6. **Myristoylation of b5R forms in the wheat germ extract and effect of myristoylation on interaction with SRP.** (A) wt b5R (lane 1), G2A (lane 2), and b5Rext (lane 3) were translated in the presence of unlabeled Met and ^{3}H-MyrCoA (see Materials and methods for details). Immunoprecipitates were run on 11% SDS–polyacrylamide gels, followed by blotting and phosphorimaging analysis. wt b5R and its extended mutant are myristoylated, whereas G2A is not. (B) Stoichiometry of in vitro myristoylation of wt b5R determined by double labeling. See Materials and methods for details on the experimental procedure. Calculation of the molar ratio of myristate to protein is based on the known specific radioactivities of the added compounds, and on the number of Met residues in the b5R sequence (8, not considering Met1). Any dilution of the specific radioactivity of ^{3}H-MyrCoA or ^{35}S-Met by the endogenous compounds is not considered. (C) Comparison of stoichiometry of in vitro myristoylation of wt b5R and b5Rext shows equal efficiency for the two proteins. wt b5R and b5Rext transcripts were translated in the wheat germ extract in the presence of ^{35}S-Met and ^{3}H-MyrCoA (21 μM). Calculation of the molar ratio of myristate to translated protein was as in B. Bars indicate the SEM (n = 5). (D) MyrCoA blunts the effect of SRP on the translation of wt b5R, but not of G2A and b5Rext. Transcripts coding for each of the three b5R forms were translated in wheat germ extract together with luciferase mRNA, 50 nM SRP, ^{35}S-Met, and the indicated concentrations of unlabeled MyrCoA. For each concentration of MyrCoA, translation efficiency is the ratio of b5R band intensity to that of luciferase in the presence of SRP normalized to the same ratio in the absence of SRP, which was set at 100. Bars indicate the SEM (n = 5). (E) Inhibition by MyrCoA of the association of wt b5R nascent chains with SRP, assessed by cross-linking. Truncated mRNAs coding for the first 108 amino acids of wt b5R (lanes 1 and 2) and G2A (lanes 6 and 7), the first 113 amino acids of b5Rext (lanes 3–5), and the first 125 residues of cytochrome b(5) (lane 8) were translated for 30 min in reticulocyte lysate with or without 75 μM MyrCoA, as indicated. RNCs were recovered by centrifugation through a high salt sucrose cushion as detailed in the Materials and methods section. For each construct, equal amounts of TCA precipitable radioactivity were cross-linked with DSS and then immunoprecipitated with an anti-SRP54 antibody, with the exception of lane 5, in which precipitation was performed with a nonimmune serum. Adducts corresponding to cross-linked products of SRP and the nascent polypeptide chains of the three forms of reductase, but not of cytochrome b(5), were detected when anti-SRP54 was used for the immunoprecipitation. Note the strong inhibitory effect of added MyrCoA on wt b5R nascent chain cross-linking (lane 2), but not on the mutant b5R forms. Exposure times were 3 d for lanes 1–5 and 12 d for lanes 6–8.

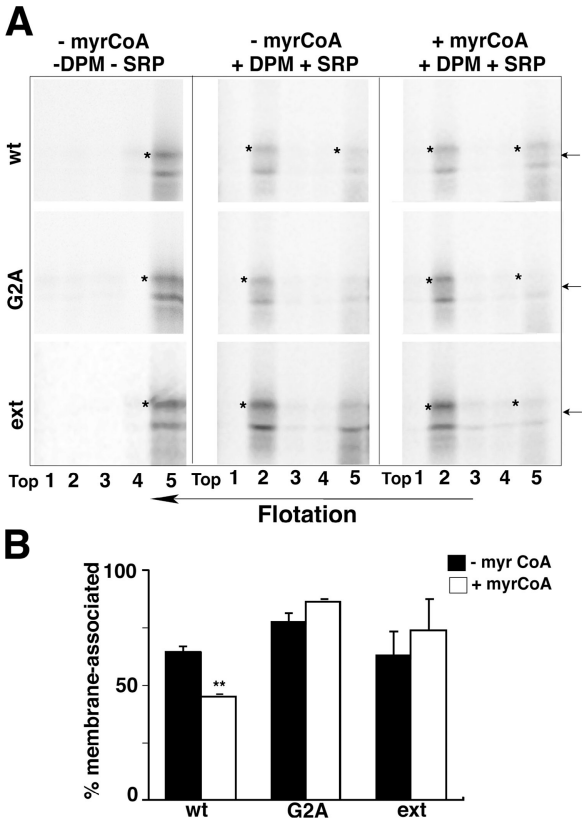

Figure 7. **Myristoylation inhibits recruitment of b5R-synthesizing polysomes to ER membranes.** (A) The truncated mRNAs coding for the NH_2-terminal portion of the three b5R forms (described in the legend to Fig. 6 E) were translated in wheat germ extract without other additions (left column), or with the addition of DPM + SRP and MyrCoA, as indicated (see Materials and methods). The translated samples were brought to 1.8 M sucrose and run on high salt-sucrose flotation gradients. TCA-precipitated fractions from the gradients were analyzed by 14% SDS-PAGE phosphorimaging. Fraction 2 contains the 0.3/1.6 M sucrose interface. Lane 5 contains the bottom fraction plus the pellet. Note the shift of the nascent chains from the bottom of the gradient, containing the free polysomes, to the 0.3/1.6 M interface, when DPM were added. When MyrCoA was present, wt b5R nascent chains were partially shifted back to the free polysome fraction. The arrow on the right indicates the position of the 14-kD size marker. (B) Quantification of three independent experiments like the one of A. The bands indicated by the asterisk in lanes 2 and 5 were quantified. Shown is the percentage recovered in lane 2 with respect to the sum of the intensities in lanes 2 + 5. Bars indicate the SEM. **, highly significant difference between the − and + MyrCoA samples (P = 0.0061 by t test).

and subjected to cross-linking with disuccinimidylsuberate (DSS). Adducts were then isolated by immunoprecipitation with anti-SRP54 antibodies and analyzed by SDS-PAGE. As shown in Fig. 6 E, in the absence of MyrCoA, all three nascent chains were cross-linked to SRP54 (lanes 1, 3, and 6), with b5Rext showing the highest efficiency. The observed cross-links were specific because (1) no adducts were precipitated by a nonimmune serum (lane 5); and (2) a truncated nascent chain lacking a signal sequence (the NH_2-terminal 125 amino acids of rabbit cytochrome b(5)) failed to cross-link to SRP (lane 8). When MyrCoA was present during translation it nearly completely blocked the subsequent cross-linking of wt b5R nascent chains to SRP (lane 2), but it was not inhibitory for b5Rext (lane 4) or G2A (lane 7).

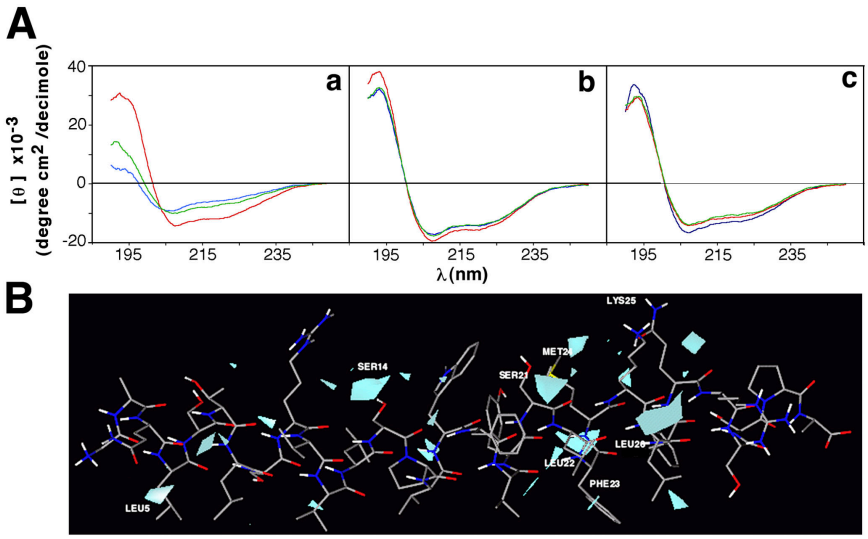

Figure 8. **Myristate stabilizes the α-helical conformation of b5R's NH_2-terminal peptide.** (A) CD spectra of b5R NH_2-terminal peptide (G2-A33). Spectra were taken for the unmodified (blue), the N-myristoylated (red), or the N-acetylated (green) peptide, diluted in water (a), 50% TFE (b), or 25 mM SDS (c). In aqueous solution the N-myristoylated peptide has a spectrum indicative of a higher α-helical content than the other two peptides. (B) Result of GRID analysis with the methyl group probe. The b5R G2-A33 peptide in α-helical conformation is represented in wireframe. Contour surfaces with favorable interaction energies of the methyl probe (threshold = −10 kJ/mol) are shown in light blue.

Myristoylation interferes with recruitment to the membrane of ribosome-b5R nascent chain complexes

The MyrCoA-induced resistance of b5R nascent chains to the action of SRP should result in the escape of the translating polysomes from recruitment to the ER membrane. To test this prediction, we translated the same truncated mRNAs used for the cross-linking experiments in the presence of dog pancreas microsomes (DPM), and investigated the effect of MyrCoA on the distribution of the resulting RNCs between free and bound polysomes by flotation on high salt sucrose gradients. As shown in Fig. 7, translation of the truncated mRNAs resulted in two major species, of which the one with slower mobility (Fig. 7 A, asterisks) presumably corresponds to the full-length truncated nascent chain. When translations were performed in the absence of added DPM, the nascent chains were quantitatively recovered in the bottom fraction and pellet of the gradient (Fig. 7 A, lane 5, left). If the translation was performed in the presence of DPM and SRP (Fig. 7 A, middle) the majority of nascent chains of all three b5R forms floated to the 1.6 M/0.3 M sucrose interface (fraction 2). As shown in the right panel of Fig. 7 A, addition of MyrCoA to the translation mix resulted in a shift of part of the translated truncated wt b5R products from the bound (fraction 2) to the free fraction (fraction 5). This effect was seen only for the wt protein, and not for the two mutants. Quantification of three separate experiments confirmed that MyrCoA decreased the fraction of wt b5R RNCs associated with DPM by ∼30% ($P < 0.01$ by *t* test), whereas it had no significant effect on the distribution of G2A and b5Rext nascent peptides (Fig. 7 B).

Effect of N-linked myristate on the conformation of b5R NH_2-terminal peptide

The above results indicate that myristoylation of b5R nascent chain interferes with SRP binding, resulting in the escape of a portion of RNCs from targeting to the ER. We hypothesized that myristoylation might affect interaction with SRP by a conformational effect on b5R's NH_2-terminal region. To test this idea, we investigated the effect of myristoylation on the secondary structure of the NH_2-terminal peptide of b5R (from G2 to A33) by circular dichroism (CD). In aqueous solution (Fig. 8 A, a), the nonmyristoylated peptide (blue trace) had a largely unordered structure (∼10% α-helix, calculated according to the equation in Chen et al., 1974), whereas the same peptide carrying N-linked myristate (red trace) showed a higher proportion (∼30%) of α-helix, as indicated by the increase in the negative peaks at 208 and 222 nm. The stabilizing effect of the attached myristate was not due simply to blockade of the NH_2 terminus because the N-acetylated G2-A33 peptide (green trace) had a spectrum similar to that of the unmodified peptide (14% helical content). Inclusion of a nonpolar solvent (trifluoroethanol [TFE]; Fig. 8 A, b) or detergent (SDS; Fig. 8 A, c) increased the α-helicity of both the unmodified and acetylated peptide, so that under these conditions all three peptides had very similar spectra.

To locate the sites within α-helical G2-A33 with highest probability for interaction with the aliphatic chain of myristic acid, we performed a computational analysis of the interaction energies between the methyl group and the α-helical peptide using the GRID program (Goodford, 1985). In Fig. 8 B, contour surfaces at which the interaction energy between peptide and methyl group is less than −10 kJ/mol are shown in light blue. The highest density of these areas is within a cluster between Ser21 and Lys25, corresponding to the most COOH-terminal part of the hydrophobic signal anchor.

Discussion

b5R, a myristoylated polypeptide anchored to the bilayer by a stretch of hydrophobic amino acids near the NH_2 terminus, is an example of a protein that is dually targeted to the MOM and the ER to carry out different functions in these two compartments. In previous work we demonstrated on the one hand that, in both the MOM and the ER, b5R is quantitatively myristoylated (Borgese and Longhi, 1990), and on the other, that the N-linked myristate is required for targeting to the former but not to the latter compartment (Borgese et al., 1996). In the present

work, we have investigated the mechanism by which this important cotranslational modification effects targeting of b5R to the MOM. On the basis of the results of our experiments, performed on three b5R forms expressed in cultured cells and in vitro, we propose that the dual MOM/ER localization of the protein occurs by a mechanism of kinetic partitioning, determined by the mutual interference between myristoylation and SRP-mediated targeting.

A hydrophobic sequence near the NH_2 terminus of a nascent chain generally acts as a signal anchor, interacting cotranslationally with SRP and thus targeting the polypeptide to the ER membrane (for review see Goder and Spiess, 2001). On the other hand, insertion of proteins into the MOM is a post-translational event (Shore et al., 1995). SRP-mediated targeting has a kinetic advantage over all post-translational targeting pathways, so that signal sequence-bearing proteins can follow post-translational targeting routes only if their binding to SRP is weak enough to allow some or all of the nascent chains to attain a critical length ("SRP window"; Rapoport et al., 1987) beyond which SRP-mediated targeting no longer occurs (Siegel and Walter, 1988). Because hydrophobicity is the principle parameter determining affinity of signal sequences for SRP (Ng et al., 1996), the MOM targeting of NH_2-terminally anchored proteins poses a theoretical problem, in that the signal anchor has to satisfy two contrasting requirements: on the one hand its hydrophobicity must be high enough to be compatible with the membrane-anchoring function, on the other, it should be weak enough to guarantee low affinity for SRP. A solution to this problem is possible only if other factors, in addition to hydrophobicity, modulate the affinity of the nascent chain for SRP. Such factors have been identified for one NH_2-terminally anchored MOM protein, TOM 20, in which charges in the regions flanking the hydrophobic stretch play a key role in SRP avoidance (Kanaji et al., 2000). In the case of b5R—whose signal anchor, although moderately hydrophobic, seems to have sufficient affinity for SRP to be quantitatively targeted to the ER (as demonstrated by the behavior of the G2A mutant)—partial escape from the SRP pathway is elegantly accomplished by a competing cotranslational event, myristoylation of the NH_2-terminal glycine.

The kinetic partitioning model for the dual ER/MOM targeting of b5R that we propose, and that is consistent with the data on the three b5R forms investigated in this paper, is illustrated in Fig. 9. Upon emergence from the ribosome, the NH_2-terminal region of wt b5R, because of its hydrophobic stretch (shown in red) and its myristoylation consensus sequence (shown in green), has the opportunity to interact both with SRP and with N-myristoyl-CoA:protein myristoyltransferase (NMT), the latter interaction preceded by removal of the NH_2-terminal Met by methionine aminopeptidase (MAP). Based on the results with b5Rext, we postulate that occupation by SRP blocks accessibility to NMT. However, different signal peptides have widely differing binding constants for SRP (Flanagan et al., 2003). The NH_2-terminal portion of wt b5R, because of its moderate affinity for SRP, will spend enough time in the unbound state to allow for its quantitative myristoylation before SRP-mediated targeting to the membrane can occur (Fig. 9, pathway 1). Once myristoylated, the affinity of the nascent peptide for SRP is further reduced so that only a fraction of the translating ribosomes manage to be targeted to the ER via the SRP pathway (Fig. 9, pathway 2). Nonetheless, because targeting to the translocation complex of a single translating ribosome will result in the association of the entire polysome with the ER, it is plausible that ribosomes translating such a membrane-associated mRNA are able to directly deliver myristoylated nascent peptide to nearby vacant translocons in an SRP-independent pathway (not depicted), resulting in the insertion of a sizeable portion of wt b5R molecules into the ER membrane.

Polysomes, of which all constituent ribosomes fail to be targeted by SRP, will remain in the free population (Fig. 9, pathway 3). Upon release from the ribosome, these chains can be post-translationally targeted to the MOM, possibly with the assistance of cytosolic chaperones (Fig. 9, pathway 4). In addition, myristoylated b5R chains that are synthesized on bound polysomes but that fail to engage a translocon will be released into the cytosol to join the pool of molecules destined for post-translational targeting to the MOM.

Our model accounts also for the behavior of b5Rext and the G2A mutant, which fail to be targeted to the MOM because of their more efficient SRP-mediated delivery to the ER. In the case of b5Rext nascent chains, the increased hydrophobicity of the signal anchor results in a strong interaction with SRP, which presumably sequesters an otherwise fully functional myristoylation consensus sequence from NMT in ~60% of the b5Rext nascent chains (Fig. 9, pathway 5). Those nascent chains that do, nonetheless, become myristoylated (Fig. 9, pathway 1) could be delivered to the ER by SRP-dependent and -independent pathways, as discussed for the wt protein. As for the G2A mutant, its interaction with SRP is similar to the one of the nonmyristoylated wt protein, but because it is not a substrate for NMT, myristoylation will not interfere with SRP-mediated delivery to the ER (Fig. 9, pathway 5).

An important question is the mechanism by which N-linked myristate interferes with SRP binding. Previous reports indicated that most signal peptides are structurally dynamic and respond to different environments by conformational changes (for review see Gierasch, 1989). Our CD investigation of the myristoylated and nonmyristoylated NH_2-terminal b5R peptide (G2-A33) revealed that the myristoylated peptide is partially α-helical in aqueous solution, whereas under the same conditions the nonmyristoylated peptide is much more unordered. Thus, N-myristoylation could decrease the affinity of b5R's signal anchor for SRP simply by constraining its conformational mobility. As suggested by the results of our GRID analysis, it is also possible that the myristoylated NH_2-terminal sequence takes on a hairpin conformation, allowing the myristoyl moiety to interact with the Ser21-Lys25 region; this conformation would probably be incompatible with SRP interaction and might also result in the physical masking of the hydrophobic residues expected to interact with the SRP 54-kD protein (Kurzchalia et al., 1986; Keenan et al., 1998).

Structural studies on other myristoylated proteins have demonstrated a helix-stabilizing effect of the N-linked fatty

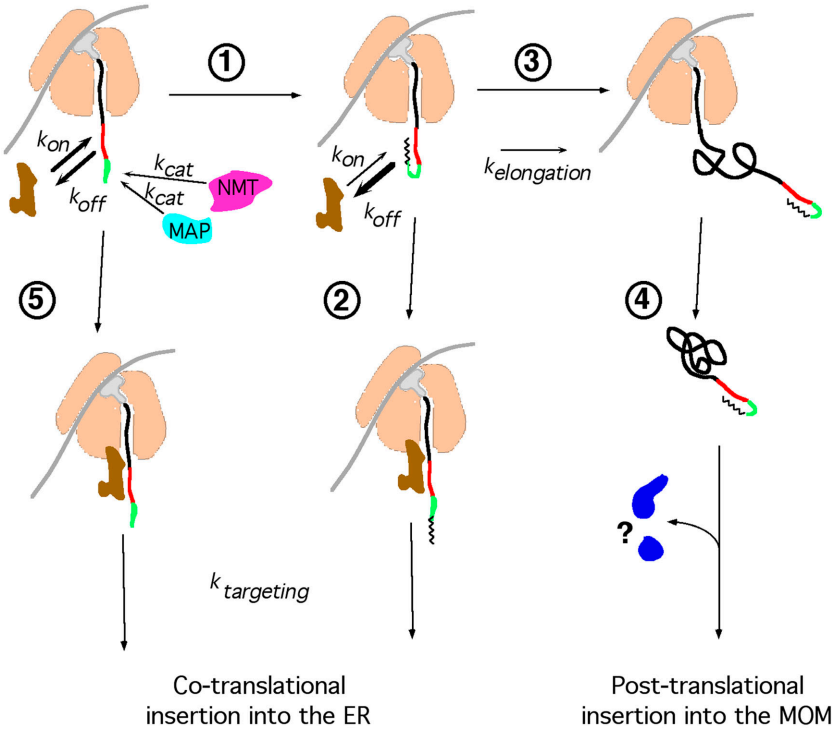

Figure 9. **A kinetic partitioning model to explain the dual ER/MOM targeting of b5R.** The different steps of alternative pathways are numbered and explained in the text. SRP is represented by the brown elongated body. The green segment of the nascent chain represents the myristoylation consensus, the red segment the hydrophobic, SRP-interacting region. The wavy black line represents the myristoyl moiety attached to the NH_2 terminus of the nascent chain. The two blue forms in pathway 4 depict unknown chaperones that might be involved in the post-translational targeting of b5R to the MOM. See Discussion for further explanation.

acid (Zheng et al., 1993; Tanaka et al., 1995). However, in these cases the myristoyl moiety lies in a hydrophobic pocket provided by several regions of the mature protein. To our knowledge, this is the first time that a stabilizing effect of N-linked myristate on a short peptide is observed, compatibly with a conformational effect of this modification on the nascent chain during the very early stages of protein synthesis.

Because it is required for the function of a number of regulatory proteins, N-myristoylation has attracted much interest since its initial discovery nearly 20 years ago (for review see Resh, 1999). In addition to simply assisting the anchorage of polypeptides to the phospholipid bilayer, this lipid modification plays highly sophisticated roles, such as participating in switch mechanisms that permit a protein to cycle in a regulated manner between membranes and the cytosol and influencing protein conformation, with consequences for protein stability, ligand binding, and protein–protein interactions. In the present paper, with the discovery that N-myristoylation can determine selection of a targeting pathway by interfering with nascent chain–SRP interaction, we have further extended the list of known functions of this interesting and highly specific lipid modification.

Materials and methods

Reagents

Goat and rabbit antisera against the hydrophilic catalytic fragment of b5R have been described previously (Borgese et al., 1996). Anti–bovine complex III antiserum, (described in Borgese et al., 1996), anti-ribophorin I, and anti-SRP54 antibodies were gifts of R. Bisson (University of Padova, Padova, Italy), G. Kreibich (New York University School of Medicine, New York, NY), and B. Dobberstein (University of Heidelberg, Heidelberg, Germany), respectively. Other antibodies were from commercial sources and are listed in the Online supplemental material.

Purified SRP (Walter and Blobel, 1983b) and DPM (Walter and Blobel, 1983a) were gifts of B. Dobberstein and U. Bach (University of Heidelberg, Heidelberg, Germany). SRP concentration was estimated by absorbance at 260 and 280 nm.

Separation of free and bound polysomes from transfected MDCK cells

MDCK II cells stably transfected with wt b5R, G2A, and b5Rext (see Fig. 1 and Online supplemental material) were fractionated by sequential detergent extraction as described by Seiser and Nicchitta (2000), with some modifications. To avoid RNA degradation standard precautions were taken, and 5% vanadyl ribonucleoside complex (Sigma-Aldrich) was present in all buffers. Cells were first permeabilized with digitonin (final concentration of 60 μg/ml; Calbiochem). After collection of the extracted material, cells were ruptured by five passages through a syringe (26G × 1/2" needle) to increase free polysome yield. The resulting homogenate was centrifuged at 3,000 *g* for 2 min followed by 17,000 *g* for 20 min in the TLA 100.3 rotor of the Optima TL ultracentrifuge (Beckman Coulter). The supernatant was combined with the initial extract. To release membrane-bound polysomes from the 17,000-*g* pellet, Triton X-100 instead of Nikkol was used. Free and bound polysomes were purified by centrifugation through a 1.6-M sucrose cushion as described by Seiser and Nicchitta (2000). After resuspension of each polysome pellet, RNA was extracted and its concentration determined by UV absorbance.

RNA blot analysis

Northern blot analysis on RNA extracted from free and bound polysome fractions was performed as described previously (Flora et al., 2000). The blot was stained with methylene blue and then sequentially hybridized with three different ^{32}P-labeled probes, prepared by random priming (Megaprime DNA labeling system; Amersham Biosciences): b5R, ribophorin I, and GAPDH. Details on the probes are given in the Online supplemental material. The blot was stripped between each hybridization step by exposing it to boiling 0.1% SDS.

In vitro transcription/translation and myristoylation

cDNA inserts in pGEM3 or pGEM4 were transcribed from the SP6 promoter after linearization with the appropriate restriction enzyme, and the resulting mRNAs were translated in the wheat germ extract (Promega) in the presence of [^{35}S]methionine, according to the instructions of the manufacturer.

For in vitro myristoylation, ^{3}H-MyrCoA was enzymatically synthesized from ^{3}H-myristic acid and Coenzyme A as described by Heuckeroth et al. (1988). In single-labeling experiments, in vitro translation was performed in the presence of 80 μM cold methionine and 1 μCi/μl ^{3}H-Myr-

CoA. The translation product was immunoprecipitated and analyzed by SDS-PAGE, followed by blotting onto nitrocellulose and exposure to the Storm Tritium screen (Amersham Biosciences).

To determine the stoichiometry between incorporated myristic acid and translated protein, mRNAs were translated in the presence of 21 μM (hot + cold) methionine (specific radioactivity of the mixture 57 Ci/mmol) and ^{3}H-MyrCoA (1 μCi/μl) diluted with unlabeled MyrCoA to the concentrations indicated in the figures. After translation for 2 h, samples were immunoprecipitated, run on SDS–polyacrylamide gels, and blotted onto nitrocellulose. The filter was exposed for sufficient time to detect the b5R band, which was then excised, solubilized with Filter-count (Packard Instrument Co.), and counted in a liquid scintillation analyzer (Tri-Carb 2100TR; Packard Instrument Co.) in dual-label mode, correcting for bleed-through of ^{35}S into the ^{3}H window.

Cross-linking of truncated nascent chains to SRP54

wt b5R, G2A, and b5Rext cDNAs were cut with DrdI within the coding sequence to produce truncated synthetic mRNAs at codon 108 for wt and G2A b5R, and at codon 113 for b5Rext. A cDNA coding for rabbit cytochrome b(5), modified to contain a unique Age1 site within codon 126, was linearized with that enzyme.

The truncated RNAs were translated in the presence of ^{35}S-Met for 30 min in reticulocyte lysate (200-μl samples), with or without the addition of 75 μM MyrCoA. After stopping translation by addition of 1 mM cycloheximide, the samples were brought to 0.125 M sucrose, 0.5 M KOAc, 5 mM $Mg(OAc)_2$, and 50 mM K-Hepes, pH 7.9, by addition of a 2× concentrated solution. RNCs were recovered after centrifugation (40,000 rpm for 2 h at 4°C in the Beckman SW 55 Ti rotor) through a 2.5-ml 0.5-M sucrose cushion, containing the same ions as above plus 1 mM DTT and 0.25 mM cycloheximide. The RNCs were resuspended in 80 μl of 0.25 M sucrose, 100 mM KOAc, 5 mM $Mg(OAc)_2$, and 50 mM K-Hepes, pH 7.9, and aliquots of the samples, containing known amounts of TCA-precipitable radioactivity (~10^6 cts/min), were incubated at 30°C for 10 min with 1 mM DSS (Pierce Chemical Co.), diluted from a 20-mM stock solution in DMSO. Cross-linking was stopped by incubation with Tris-HCl, pH 8.5, added to a final concentration of 100 mM, for 20 min at 30°C. After a further incubation (for 20 min at 30°C) with 0.1 mg/ml RNase A, samples were immunoprecipitated with anti-SRP54 antibodies under denaturing conditions (Abell et al., 2004).

Flotation of nascent chain–ribosome–membrane complexes

The b5R truncated mRNAs described for the cross-linking experiments were translated in wheat germ extract (10-μl sample volume) for 30 min in the presence or absence of DPM (3.3 equivalents) together with SRP (50 nM), or DPM, SRP, and MyrCoA (70 μM). After blocking protein synthesis with 1 mM cycloheximide, free and membrane-bound RNCs were separated by flotation in high salt sucrose gradients as described by Belin et al. (1996). Fractions were precipitated with TCA and analyzed by SDS-PAGE phosphorimaging.

Peptide synthesis and CD

The synthetic 32mer (G2-A33) peptide representing the NH_2-terminal domain of rat b5R (GAQLSTLSRVVLSPVWFVYSLFMKLFQRSSPA) was synthesized by the stepwise solid phase Fmoc method (Fields and Noble, 1990), as described previously (Consonni et al., 2003). After completion of peptide chain assembly, one aliquot was left unmodified, whereas two aliquots were either N-acetylated or N-myristoylated, as detailed in the Online supplemental materials and methods section.

CD spectra were collected at 22°C in a cuvette with a path length of 0.1 cm, using a spectropolarimeter (J-810; Jasco). Peptides, dissolved in 50% TFE, were diluted 20-fold to a concentration of 0.1 mg/ml, either in water, in 50% TFE, or in 25 mM SDS. The pH of all dilutions was checked and found to be close to 7. Each shown spectrum is the average of 3–5 baseline-subtracted scans. The helical population was estimated from the measured mean residue ellipticity at 222 nm, using the equation $fH = ([\theta]222 - 2340)/30300$ (Chen et al., 1974).

Computational analysis of G2-A33 peptide

A computational analysis of the interaction energies of the methyl group with the G2-A33 peptide in α-helical conformation was performed with the GRID program (Goodford, 1985). The peptide, built in zwitterionic α-helical conformation was energy minimized with AMBER force field in the Gibbs Born/Surface Area water-implicit model of solvation, and analyzed using the GRID methodology. Areas with an interaction energy lower than −10 kJ/mol were displayed as contours on the α-helical peptide structure.

Other techniques

Immunofluorescent specimens were observed under a laser confocal microscope (MRC 1024 ES; Bio-Rad Laboratories), with the use of a 60× oil immersion objective (N.A. 1.4; Nikon). Polyacrylamide gels containing radioactively labeled samples were imaged with the Storm phosphorimager (Amersham Biosciences) and band intensities were quantified with ImageQuant software (Amersham Biosciences). Immunofluorescence and gel images were prepared for the illustrations with the use of Adobe Photoshop software. Plasmid constructions and cell culture were performed by standard procedures that are described in the Online supplemental material.

Online supplemental material

The supplemental materials and methods section gives details on sources of reagents, and describes cell fractionation, immunoblotting, enzyme assay, plasmid constructions, transfection of cultured cells, ^{32}P-labeled probes for Southern blots, and peptide synthesis and characterization. Fig. S1 shows an analysis of b5R enzyme activity in the transfected cell lines, and the results of cell fractionation experiments. Online supplemental material available at http://www.jcb.org/cgi/content/full/jcb.200407082/DC1.

We thank Gert Kreibich for his gift of antibodies and ribophorin I cDNA and Roberto Bisson for anti-complex III antiserum. We are particularly indebted to Bernhard Dobberstein and Ute Bach for their gift of SRP, microsomes, and anti-SRP54 antibodies and to Bernhard Dobberstein and Ramanujan Hegde for critically reading the manuscript. We are also grateful to Emanuela Pedrazzini for helpful suggestions.

This work was supported by a grant from Telethon (E.0734) and from the MURST (COFIN 2002) to N. Borgese.

Submitted: 13 July 2004
Accepted: 10 January 2005

References

Abell, B.M., M.R. Pool, O. Schlenker, I. Sinning, and S. High. 2004. Signal recognition particle mediates post-translational targeting in eukaryotes. *EMBO J.* 23:2755–2764.

Adams, J.M., and S. Cory. 2001. Life-or-death decisions by the Bcl-2 protein family. *Trends Biochem. Sci.* 26:61–66.

Belin, D., S. Bost, J.-D. Vassalli, and K. Strub. 1996. A two-step recognition of signal sequences determines the translocation efficiency of proteins. *EMBO J.* 15:468–478.

Bernardi, P., and G.F. Azzone. 1981. Cytochrome *c* as an electron shuttle between the outer and inner mitochondrial membranes. *J. Biol. Chem.* 256:7187–7192.

Borgese, N., and S. Gaetani. 1980. Site of synthesis of rat liver NADH-cytochrome b_5 reductase, an integral membrane protein. *FEBS Lett.* 112:216–220.

Borgese, N., and R. Longhi. 1990. Both the outer mitochondrial membrane and the microsomal forms of cytochrome b_5 reductase contain covalently bound myristic acid. Quantitative analysis on the polyvinylidene difluoride-immobilized proteins. *Biochem. J.* 266:341–347.

Borgese, N., A. D'Arrigo, M. De Silvestris, and G. Pietrini. 1993. NADH-cytochrome b_5 reductase and cytochrome b_5—the problem of postranslational targeting to the endoplasmic reticulum. *In* Subcellular Biochemistry. Vol. 21. N. Borgese and J.R. Harris, editors. Plenum Press, New York. 313–341.

Borgese, N., D. Aggujaro, P. Carrera, G. Pietrini, and M. Bassetti. 1996. A role for N-myristoylation in protein targeting: NADH-cytochrome b_5 reductase requires myristic acid for association with outer mitochondrial but not endoplasmic reticulum membranes. *J. Cell Biol.* 135:1501–1513.

Chen, Y.H., J.T. Yang, and K.H. Chau. 1974. Determination of the helix and beta form of proteins in aqueous solution by circular dichroism. *Biochemistry.* 13:3350–3359.

Consonni, R., I. Arosio, T. Recca, R. Longhi, G. Colombo, and M. Vanoni. 2003. Structure determination and dynamics of peptides overlapping the catalytic hairpin of the Ras-GEF $Cdc25^{Mm}$. *Biochemistry.* 42:12154–12162.

Cornette, J.L., K.B. Cease, H. Margalit, J.L. Spouge, J.A. Berzofsky, and C. DeLisi. 1987. Hydrophobicity scales and computational techniques for detecting amphipathic structures in proteins. *J. Mol. Biol.* 195:659–685.

Danpure, C.J. 1995. How can the products of a single gene be localized to more than one intracellular compartment? *Trends Cell Biol.* 5:230–238.

Deichaite, I., L.P. Casson, H.P. Ling, and M.D. Resh. 1988. In vitro synthesis of pp60v-src: myristylation in a cell-free system. *Mol. Cell. Biol.* 8:4295–4301.

Fields, G.B., and R.L. Noble. 1990. Solid phase peptide synthesis utilizing 9-fluo-

renylmethoxycarbonyl amino acids. *Int. J. Pept. Protein Res.* 35:161–214.

Flanagan, J.J., J.C. Chen, Y. Miao, Y. Shao, J. Lin, P.E. Bock, and A.E. Johnson. 2003. Signal recognition particle binds to ribosome-bound signal sequences with fluorescence-detected subnanomolar affinity that does not diminish as the nascent chain lengthens. *J. Biol. Chem.* 278:18628–18637.

Flora, A., R. Schulz, R. Benfante, E. Battaglioli, S. Terzano, F. Clementi, and D. Fornasari. 2000. Neuronal and extraneuronal expression and regulation of the human α5 nicotinic receptor subunit gene. *J. Neurochem.* 75:18–27.

Gierasch, L.M. 1989. Signal sequences. *Biochemistry.* 28:923–930.

Goder, V., and M. Spiess. 2001. Topogenesis of membrane proteins: determinants and dynamics. *FEBS Lett.* 504:87–93.

Goodford, P.J. 1985. A computational procedure for determining energetically favorable binding sites on biologically important macromolecules. *J. Med. Chem.* 28:849–857.

Harnik-Ort, V., K. Prakash, E. Marcantonio, D.R. Colman, M.G. Rosenfeld, M. Adesnik, D.D. Sabatini, and G. Kreibich. 1987. Isolation and characterization of cDNA clones for rat ribophorin I: complete coding sequence and in vitro synthesis and insertion of the encoded product into endoplasmic reticulum membranes. *J. Cell Biol.* 104:855–863.

Heuckeroth, R.O., D.A. Towler, S.P. Adams, L. Glaser, and J.I. Gordon. 1988. 11-(Ethylthio)undecanoic acid. A myristic acid analogue of altered hydrophobicity which is functional for peptide N-myristoylation with wheat germ and yeast acyltransferase. *J. Biol. Chem.* 263:2127–2133.

Ito, A., S. Hayashi, and T. Yoshida. 1981. Participation of a cytochrome b_5-like hemoprotein of outer mitochondrial membrane (OM cytochrome b) in NADH-semidehydroascorbic acid reductase activity of rat liver. *Biochem. Biophys. Res. Commun.* 101:591–598.

Jaffé, E.R., and D.E. Hultquist. 1995. Cytochrome b_5 reductase deficiency and enzymatic hereditary methemoglobinemia. *In* The Metabolic and Molecular Bases of Inherited Disease. 7th ed. C.R. Scriver, A.L. Beaudet, W.S. Sly, and D. Valle, editors. McGraw-Hill, New York. 3399–3415.

Kanaji, S., J. Iwahashi, Y. Kida, M. Sakaguchi, and K. Mihara. 2000. Characterization of the signal that directs Tom20 to the mitochondrial outer membrane. *J. Cell Biol.* 151:277–288.

Keenan, R.J., D.M. Freymann, P. Walter, and R.M. Stroud. 1998. Crystal structure of the signal sequence binding subunit of the signal recognition particle. *Cell.* 94:181–191.

Kim, S.J., and R.S. Hegde. 2002. Cotranslational partitioning of nascent prion protein into multiple populations at the translocation channel. *Mol. Biol. Cell.* 13:3775–3786.

Kurzchalia, T.V., M. Wiedmann, A.S. Girshovich, E.S. Bochkareva, H. Bielka, and T.A. Rapoport. 1986. The signal sequence of nascent preprolactin interacts with the 54K polypeptide of the signal recognition particle. *Nature.* 320:634–636.

Ng, D.T., J.D. Brown, and P. Walter. 1996. Signal sequences specify the targeting route to the endoplasmic reticulum membrane. *J. Cell Biol.* 134:269–278.

Okada, Y., A.B. Frey, R.M. Guenthner, F. Oesch, D.D. Sabatini, and G. Kreibich. 1982. Studies on the biosynthesis of microsomal membrane proteins. Site of synthesis and mode of insertion of cytochrome b_5, cytochrome b_5 reductase, cytochrome P-450 reductase and epoxide hydrolase. *Eur. J. Biochem.* 122:393–402.

Ozols, J., S.A. Carr, and P. Strittmatter. 1984. Identification of the NH_2-terminal blocking group of NADH-cytochrome b_5 reductase as myristic acid and the complete amino acid sequence of the membrane-binding domain. *J. Biol. Chem.* 259:13349–13354.

Pietrini, G., D. Aggujaro, P. Carrera, J. Malisco, A. Vitale, and N. Borgese. 1992. A single mRNA, transcribed from an alternative, erythroid-specific, promoter, codes for two non-myristylated forms of NADH-cytochrome b_5 reductase. *J. Cell Biol.* 117:975–986.

Rapoport, T.A., R. Heinrich, P. Walter, and T. Schulmeister. 1987. Mathematical modeling of the effects of the signal recognition particle on translation and translocation of proteins across the endoplasmic reticulum membrane. *J. Mol. Biol.* 195:621–636.

Resh, M.D. 1999. Fatty acylation of proteins: new insights into membrane targeting of myristoylated and palmitoylated proteins. *Biochim. Biophys. Acta.* 1451:1–16.

Seiser, R.M., and C.V. Nicchitta. 2000. The fate of membrane-bound ribosomes following the termination of protein synthesis. *J. Biol. Chem.* 275:33820–33827.

Shirabe, K., M.T. Landi, M. Takeshita, G. Uziel, E. Fedrizzi, and N. Borgese. 1995. A novel point mutation in a 3′ splice site of the NADH-cytochrome b_5 gene results in immunologically undetectable enzyme and impaired NADH-dependent ascorbate regeneration in cultured fibroblasts of a patient with type II hereditary methemoglobinemia. *Am. J. Hum. Genet.* 57:302–310.

Shore, G.C., H.M. McBride, D.G. Millar, N.A.E. Steenaart, and M. Nguyen. 1995. Import and insertion of proteins into the mitochondrial outer membrane. *Eur. J. Biochem.* 227:9–18.

Siegel, V., and P. Walter. 1988. The affinity of signal recognition particle for presecretory proteins is dependent on nascent chain length. *EMBO J.* 7:1769–1775.

Strittmatter, P., J.M. Kittler, J.E. Coghill, and J. Ozols. 1993. Interaction of non-myristoylated NADH-cytochrome b_5 reductase with cytochrome b_5-dimyristoylphosphatidylcholine vesicles. *J. Biol. Chem.* 268:23168–23171.

Tanaka, T., J.B. Ames, T.S. Harvey, L. Stryer, and M. Ikura. 1995. Sequestration of the membrane-targeting myristoyl group of recoverin in the calcium-free state. *Nature.* 376:444–447.

Walter, P., and G. Blobel. 1983a. Preparation of microsomal membranes for cotranslational protein translocation. *Methods Enzymol.* 96:84–93.

Walter, P., and G. Blobel. 1983b. Signal recognition particle: a ribonucleoprotein required for cotranslational translocation of proteins, isolation and properties. *Methods Enzymol.* 96:682–691.

Zheng, J., D.R. Knighton, N.-H. Xuong, S.S. Taylor, J.M. Sowadski, and L.F. Ten Eyck. 1993. Crystal structures of the myristylated catalytic subunit of cAMP-dependent protein kinase reveal open and closed conformations. *Protein Sci.* 2:1559–1573.